Proceedings of the ASME 2010 3rd Joint US-European Fluids Engineering Summer Meeting and 8th International Conference on Nanochannels, Microchannels, and Minichannels
FEDSM-ICNMM2010
August 1-5, 2010, Montreal, Canada

FEDSM-ICNMM2010-30351

EXTENDED SELF-SIMILARITY IN DRAG-REDUCED TURBULENT FLOW OF VISCOELASTIC FLUID

Feng-Chen Li, Hong-Na Zhang, Wei-Hua Cai, Juan-Cheng Yang
School of Energy Science and Engineering, Harbin Institute of Technology
Harbin 150001, Heilongjiang, China

ABSTRACT

Direct numerical simulations (DNS) have been performed for drag-reduced turbulent channel flow with surfactant additives and forced homogeneous isotropic turbulence with polymer additives. Giesekus constitutive equation and finite extensible nonlinear elastic model with Peterlin closure were used to describe the elastic stress tensor for both cases, respectively. For comparison, DNS of water flows for both cases were also performed. Based on the DNS data, the extended self-similarity (ESS) of turbulence scaling law is investigated for water and viscoelastic fluids in turbulent channel flow and forced homogeneous isotropic turbulence. It is obtained that ESS still holds for drag-reduced turbulent flows of viscoelastic fluids. In viscoelastic fluid flows, the regions at which $\delta u(r) \propto r$ and $S_p(r) \propto S_3(r)^{\zeta(p)}$ with $\zeta(p) = p/3$, where r is the scale length, $\delta u(r)$ is the longitudinal velocity difference along r and $S_p(r)$ is the pth-order moment of velocity increments, in the K41 (Kolmogorov theory) - fashioned plots and ESS-fashioned plots, respectively, are all broadened to larger scale for all the investigated cases.

INTRODUCTION

Scaling of the structure functions in turbulent flows plays very important roles in the statistical physics of turbulence and the existence of scaling is an indication of scale invariance in turbulence. The pth-order structure function is defined as the pth-order moment of velocity increments at the scale r,

$$S_p(r) = \left\langle \left|\delta u(r)\right|^p \right\rangle = \left\langle \left|u(x+r) - u(x)\right|^p \right\rangle \quad (1)$$

where $\langle \cdots \rangle$ represents ensemble average and u is the longitudinal velocity component along r. At a scale r satisfying $L > r \gg \eta$ where L is the integral scale and $\eta = \left(\nu^3/\varepsilon\right)^{1/4}$, the scaling law of structure function might exist,

$$S_p(r) \propto r^{\zeta(p)} \quad (2)$$

The Kolmogorov theory (K41) gives the scaling exponent $\zeta(p) = p/3$, which has been modified with consideration of the intermittency of turbulence.

The scaling law is obvious at a range of scale, i.e. inertial range, only for high-Reynolds-number turbulent flow. At low or moderate Reynolds number, $\mathrm{Re} = U_0 L/\nu$, the scaling law is either indiscernible or valid in a very small internal of r. Benzi et al. [1] proposed the so-called extended self-similarity (ESS) establishing an extended region of the observed scale similarity. Formally, ESS refers to as,

$$S_p(r) \propto S_q(r)^{\zeta(p)/\zeta(q)} \quad (3)$$

Since in K41, $\zeta(3) = 1$, $q = 3$ is usually used in ESS,

$$S_p(r) \propto S_3(r)^{\zeta(p)} \quad (4)$$

Benzi et al. [1-3] showed that, with the same scaling exponents of fully developed turbulence, Eq. (4) is valid not only at high Re but also at moderate low Re with invisible inertial range according to Eq. (2).

With addition of a minute amount of long-chain polymer or some kind of surfactant additives into a normal Newtonian liquid such as water turbulent flow may cause a dramatic reduction of frictional drag, which is named turbulent drag reduction (DR) [4-6]. However, the drag-reduced turbulent flow by drag-reducing additives is still in turbulent flow state, but with modified turbulence characteristics. In this paper, we performed direct numerical simulation (DNS) for a drag-reducing channel flow of surfactant solution and a forcing homogeneous isotropic turbulence (FHIT) with drag-reducing polymer additives. We are aiming at further understanding turbulent drag reduction phenomenon as well as shedding light on the essence of turbulence through exploring the scaling properties of the structure functions in drag-reduced turbulent flows based on DNS database.

NOMENCLATURE

$\mathbf{C}$	conformation tensor (1/N)
E	turbulent energy spectrum (m^2/s^2)
$\mathbf{F}$	additional body force (N)
$f(r)$	non-linear spring force (N)
h	channel height (m)
$\mathbf{I}$	unit tensor
L	integral scale (m)
L_x	computation domain size in x direction (m)
L_y	computation domain size in y direction (m)
L_z	computation domain size in z direction (m)
l	extension length of polymer (m)
l_m	maximum possible extension of polymer (m)
$p(\mathbf{x},t)$	local pressure (Pa)
R	period cubic domain size (m)
Re	Reynolds number
r	scale length (m)
$\mathbf{S}$	rate-of-strain tensor (1/s)
$S_p(r)$	pth-order structure function
$\mathbf{T}$	stress tensor (Pa)
U_0	characteristic velocity of the flow (m/s)
$\mathbf{u}(\mathbf{x},t)$	velocity vector (m/s)
u	velocity component along r (m/s)
Wi	Wessenberg number
y	wall-normal coordinate (m)
Greek Symbols	
α	mobility factor
β	viscosity ratio
δ_{ij}	Kroneker delta
ε	turbulent kinetic energy dissipation rate (m^2/s^3)
η	Kolmogorov length scale (m)
λ	Taylor micro scale (m)
ν	kinematic viscosity (m^2/s)
$\zeta(p)$	scaling exponent
ρ	density (kg/m^3)
τ_p	relaxation time of polymer (s)
ξ	total kinetic energy (m^2/s^2)
Superscripts and/or subscripts	
p	viscoelastic polymer or surfactant additives
s	solvent

DESCRIPTION OF NUMERICAL SIMULATION

We investigate viscoelastic fluid turbulent flows which can be described by the continuity and generalized momentum equations including the viscoelastic-additives interaction coupled with generalized constitutive model as follows:

$$\nabla\cdot\mathbf{u}=0 \tag{5}$$

$$\frac{\partial\mathbf{u}}{\partial t}+\mathbf{u}\cdot\nabla\mathbf{u}=-\frac{1}{\rho}\nabla p+\frac{1}{\rho}\nabla\cdot\mathbf{T}^{[s]}+\frac{1}{\rho}\nabla\cdot\mathbf{T}^{[p]}+\mathbf{F} \tag{6}$$

$$\frac{\partial\mathbf{C}}{\partial t}+\mathbf{u}\cdot\nabla\mathbf{C}=\mathbf{C}\cdot\nabla\mathbf{u}+\nabla\mathbf{u}^T\cdot\mathbf{C}-\frac{1}{\tau_p}\left[\mathbf{I}+\alpha(\mathbf{C}-\mathbf{I})\right]\cdot\left[f(l)\mathbf{C}-\mathbf{I}\right] \tag{7}$$

$$\mathbf{T}^{[s]}=2\rho\nu^{[s]}\mathbf{S},\quad \mathbf{S}=\frac{1}{2}(\nabla\mathbf{u}+\nabla\mathbf{u}^T),\quad \mathbf{T}^{[p]}=\rho\nu^{[p]}(f(l)\mathbf{C}-\mathbf{I})/\tau_p \tag{8}$$

In the present study Giesekus model (for viscoelastic surfactant solution) with $\alpha=0.001, f(l)=1$ and finite extensible nonlinear elastic model (for viscoelastic polymer solution) with Peterlin closure (FENE-P) with $\alpha=0, f(l)=\left(l_m^2-3\right)/\left(l_m^2-l^2\right)$ [7] are adopted in channel turbulent flow and FHIT, respectively. We performed DNS for incompressible fluid with and without viscoelastic additives in both channel turbulent flow and FHIT.

Channel turbulent flow

The simulation of channel turbulent flow is based on the dimensionless governing equations for a fully developed turbulent channel flow with computation domain size of $L_x\times L_y\times L_z=10h\times 2h\times 5h$, in which x, y, and z represents the streamwise, normal and spanwise directions, respectively. During the process of non-dimensionalization the following nondimensional variables are introduced: $x_i^*=\frac{x_i}{h}$, $t^*=\frac{t}{h/u_\tau}$, $u_i^+=\frac{u_i}{u_\tau}$, $p^+=\frac{p}{\rho u_\tau^2}$, $c_{ij}^+=c_{ij}$, $\mathrm{Re}_\tau=\frac{\rho u_\tau h}{\nu^{[s]}+\nu^{[p]}}$, $Wi_\tau=\frac{\tau_p\rho u_\tau^2}{\nu^{[s]}+\nu^{[p]}}$, where u_τ is the friction velocity; Re_τ the Reynolds number based on u_τ and Wi_τ the Weissenberg number based on u_τ indicating the elastic strength of flow. The periodic boundary conditions in streamwise and spanwise direction and nonslip boundary condition for the top and bottom wall are used in the simulation.

The finite difference schemes is adopted to discretize the governing equations based on a staggered grid system (64^3) with velocity components at the cell interfaces and other variables at the nodes. MINMOD scheme is used for discretization of the convective term in the constitutive equation and second order central difference scheme for other spatial terms. For the time integration, Adams-Bashforth scheme is employed. More details, including the grid-dependence analysis, can be found in Refs. [8-10].

The simulation spans 2×10^5 time steps, corresponding to about 60 streamwise recirculation times. For every time step, the streamwise velocity was extracted at three different locations which are inside the viscous sublayer right above the bottom wall, within the transition layer and the logarithmic layer, respectively. The locations and the parameters in different cases are listed in Table I. In table I, y^+ is the normal-to-wall distance normalized with u_τ and the solvent viscosity ν, i.e., $y^+=yu_\tau/\nu=\mathrm{Re}_\tau y/h$, and $\beta=\nu^{[s]}/\left(\nu^{[s]}+\nu^{[p]}\right)$ is a dimensionless measure of dilute surfactant solution concentration, and smaller β corresponds to denser surfactant solution).

Table I Locations of sampling points and the parameters in different cases for channel flow

Locations			Wi_τ	Re_τ	Re_m	β	DR
y^+=4	y^+=16	y^+=232	0	240	7192	0	0
y^+=4	y^+=16	y^+=232	50	240	10645	0.5	43%

Forcing homogeneous and isotropic turbulence

To solve Eq.(6), a standard pseudo-spectral code with 96^3 collocation points in the periodic cubic domain of size $R = 2\pi$ is used for spatial discretization with all the nonlinear terms fully de-aliased by the 3/2 rule. For time advancement a second-order Adams-Bashforth scheme is adopted. To solve Eq.(7), a second-order central difference scheme are used except for convective term using the second-order Kurganov-Tadmor (KT) scheme to ensure the symmetric and positive definite (SPD) property of polymer conformation tensor [11] for spatial discretization and for time marching a second-order Adams-Bashforth scheme is adopted.

The initial velocity field is obtained based on Rogallo's procedure [7, 12] and the initial energy spectrum $E_0(k) = 0.01k^4 \exp(-0.14k^2)$. For initial conformation field, polymers are assumed non-stretched, corresponding to $C_{ij}^0(x,y,z) = \delta_{ij}$ [13, 14]. In Fourier space, the turbulent kinetic energy spectrum $E(k,t) = \sum_{k-1/2<k\le k+1/2} \left|\mathbf{u}_k(t)\right|^2/2$, the energy-dissipation rate $\varepsilon(t) = \nu^{[s]}\sum_k k^2 E(k,t)$ and the total kinetic energy $\xi(t) = \sum_k E(k,t)$. The stationary isotropic turbulence is obtained by adding an additional force which keeps the total energy of the first two wavenumbers constant in time, $E_1 \doteq 0.31$ and $E_2 \doteq 0.13$, and the details can be found in Refs. [15, 16]. The Taylor microscale is defined as $\lambda = \sqrt{15\nu^{[s]} < u^2 > / \varepsilon(t)}$, where $< u^2 >= 2\xi(t)/3$ is turbulent fluctuation intensity. Taylor-microscale Reynolds number Re_λ and the Weissenberg number Wi are defined as $\mathrm{Re}_\lambda = \sqrt{20}\xi^N / \sqrt{3\nu^{[s]}\varepsilon^N}$ and $\mathrm{Wi} = \tau_p \sqrt{\varepsilon^N / \nu^{[s]}}$ [14], respectively, where the superscript "N" represents the Newtonian fluid case. Simulations are based on the following parameters: $\mathrm{Re}_\lambda = 46$, $\mathrm{Wi} = 0.27$, $\tau_p = 0.1$ s, $\beta = 0.6$ for polymer solution case and $\mathrm{Re}_\lambda = 46$ for Newtonian fluid case.

During the simulation of FHIT 10^5 time series of velocity information at the center of computational domain is obtained to satisfy the statistical requirement.

RESULTS AND DISCUSSIONS

DNS has been performed for drag-reducing turbulent channel flow of surfactant solution and FHIT with polymer additives. For channel flow, a significant DR (43%) has been obtained at the flow conditions simulated. The overall characteristics of DR, statistical quantities and flow structures modified by the drag-reducing additives will not be shown here. For FHIT, although the simulated Wi was relatively small $\mathrm{Wi} = 0.27$, we have obtained a significant polymer effect on the turbulence characteristics of FHIT. Fig. 1 gives such polymer effect as an example. It shows that in FHIT with polymer additives, the total turbulent kinetic energy has been evidently decreased as compared with Newtonian fluid case, and the kinetic energy spectrum is also greatly altered. Further analyses are then carried out on the DNS databases for drag-reduced channel flow and FHIT with polymer additives, emphasizing on the scaling properties of structure functions, and its linkage with DR mechanism.

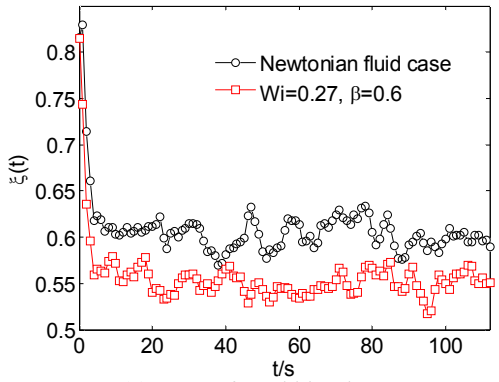

(a) trace of total kinetic energy

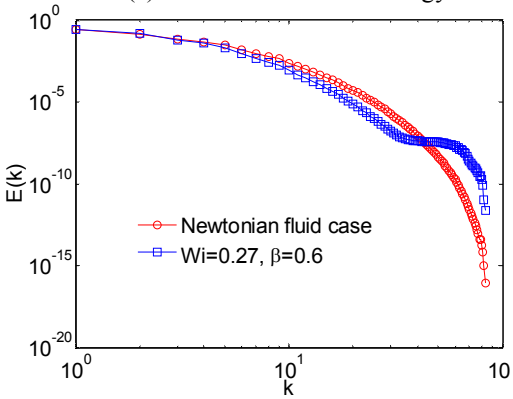

(b) turbulent kinetic energy spectrum

Fig. 1 Polymer effects on the characteristics of FHIT

We at first show $S_3(r)$ in a fashion of K41 scaling law, i.e., plotting $S_3(r)$ versus $\log_{10}(r)$ for all the simulated cases, as shown in Fig. 2. As expected, at the moderate small Reynolds number in the present DNS study, no visible inertial range at which $S_3(r) \propto 1$ can be observed from Fig. 2. At small scale r (approximately below 30η for channel flow and below 3η for FHIT, respectively), the velocity difference is regular for both Newtonian fluid and drag-reducing viscoelastic fluid flows, i.e., $\delta u(r) \propto r$ and a clear slope 3 can be obtained for $S_3(r)$ against $\log_{10}(r)$. The difference between Newtonian fluid and viscoelastic fluid cases is that the range of this small scale r at which $\delta u(r) \propto r$ is enlarged in the latter, which can be seen from the parallel shift of the curve to larger r as plotted in Fig. 2. This is conceivable since the micro structures formed in viscoelastic fluid interacts with turbulent eddies and tends to smooth the velocity fluctuations, making the region of regular behavior broader. For other structure functions in different orders, similar phenomena can be observed for Newtonian fluid and viscoelastic fluid cases.

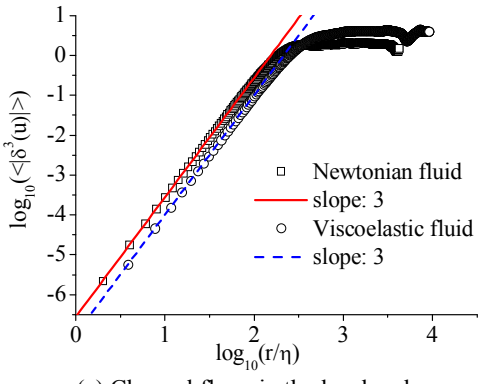

(a) Channel flow: in the log-law layer

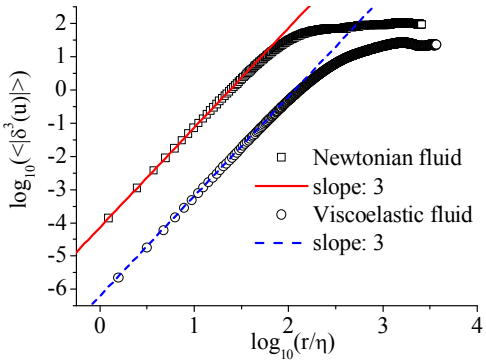

(b) Channel flow: in the transition layer

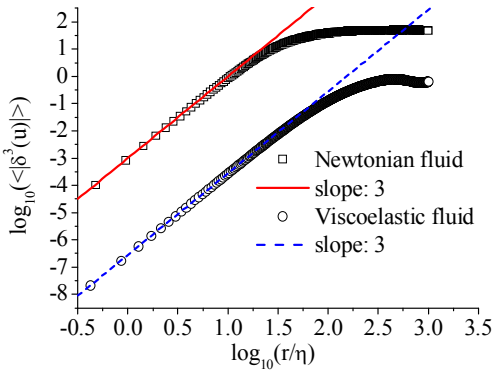

(c) Channel flow: in the viscous layer

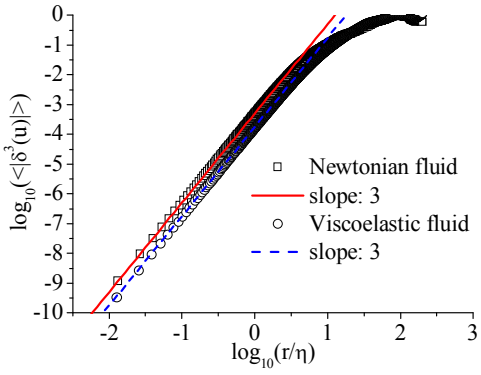

(d) FHIT

Fig. 2 Log-log plot of $S_3(r)$ vs r for channel flow and FHIT

The structure functions in ESS fashion, i.e., plotting $\log_{10}\left(S_p(r)\right)$ versus $\log_{10}\left(S_3(r)\right)$ are then plotted in Fig. 3. For clarity, only $S_2(r)$ and $S_8(r)$ are provided for all the cases. In our studied cases, two distinct phenomena can be noticed from the ESS fashioned plots. Firstly, we have not observed any clear region of anomalous scaling (with scaling exponent different from $p/3$) corresponding to ESS as discussed by Benzi et al. [2] for their wind-tunnel experiments on the grid turbulence behind cylinders, but only the obvious region from the smallest scale at which $\zeta(p)=p/3$, in both turbulent channel flow and FHIT for Newtonian fluid flow and drag-reducing flows with additives, respectively. If there is the so-called anomalous ESS scaling region as pointed out by Benzi et al. [2], it might be immersed in the extension of regular region (as shown in Fig. 2 for $S_3(r)$ versus $\log_{10}(r)$) and with a too slight slope difference to be distinguished. That's why we hesitated to plot such fitted slope beyond the end of the regular region. However, we prefer to argue that the broader linear region appeared in the plots of $\log_{10}\left(S_p(r)\right)$ versus $\log_{10}\left(S_3(r)\right)$ as shown in Fig. 3 has been a kind of ESS behavior, as compared with the narrower linear region shown in Fig. 2 for $S_3(r)$ versus $\log_{10}(r)$. This issue will be explored in much more detail in the near future, by investigating more cases. Secondly, we found that the region at which $S_p(r)\propto S_3(r)^{p/3}$ has been greatly broadened to larger scale by the viscoelastic additives for all the inspected cases. This is more important for our purpose of further understanding the DR mechanism in both drag-reduced wall flow and FHIT with drag-reducing additives. Through careful investigation of the valid range of $p/3$ slope plotted in Fig. 3, the largest r/η, designated as $(r/\eta)_T$ below which $\zeta(p)=p/3$ is apparent, is obtained for all the cases from the original data of Fig. 2, as listed in Table II, where "N" indicates Newtonian fluid case and "V" represents viscoelastic fluid case, respectively. It can be seen that the values of $(r/\eta)_T$ have been all greatly enlarged for structure functions $S_2(r)$ and $S_8(r)$ investigated here (We calculated the structure functions up to 8th-order due to the limitation of sampling space of the data. For other structure functions, similar phenomena have been obtained) at the 3 positions in turbulent channel flow and in FHIT for viscoelastic fluid case.

The aforementioned analyses indicate that the influence of drag-reducing additives on the characteristics of ESS or the scaling properties of turbulence is distinct. From the viewpoint of DR mechanism, the most salient feature emerged in drag-

Table II Length scale $(r/\eta)_T$ at which the validation of $\zeta(p)=p/3$ for ESS $S_p(r)\propto S_3(r)^{\zeta(p)}$ ends.

Cases \ $(r/\eta)_T$		Channel flow			FHIT
		Log-law layer	Transition layer	Viscous layer	
$S_2(r)$	N	186.2	22.4	6.3	1.4
	V	407.4	42.7	34.7	2.3
$S_8(r)$	N	61.7	10.0	3.4	0.7
	V	223.9	18.6	18.2	1.4

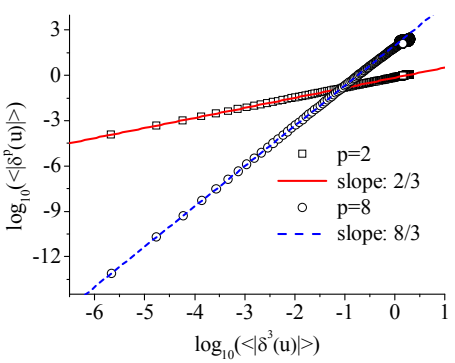

(i) Newtonian fluid flow

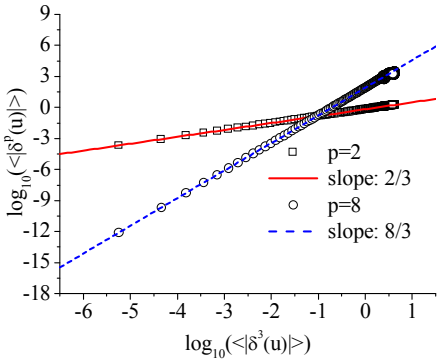

(ii) Drag reducing flow

(a) Channel flow: in the log-law layer

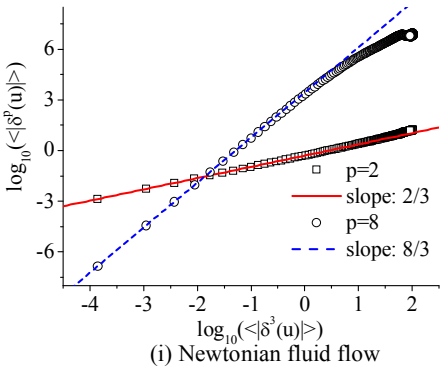

(i) Newtonian fluid flow

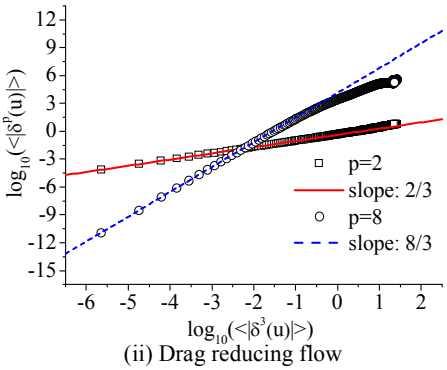

(ii) Drag reducing flow

(b) Channel flow: in the transition layer

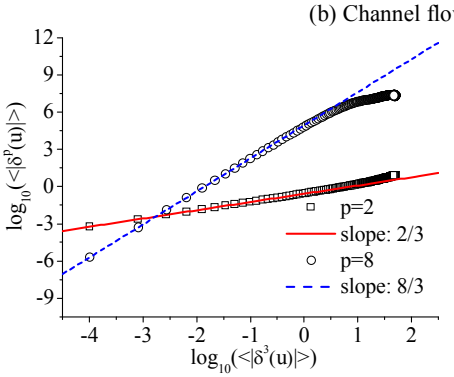

(i) Newtonian fluid flow

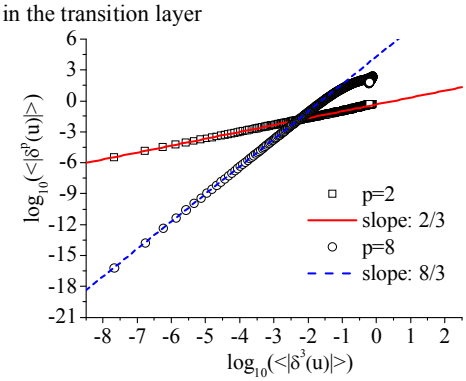

(ii) Drag reducing flow

(c) Channel flow: in the viscous layer

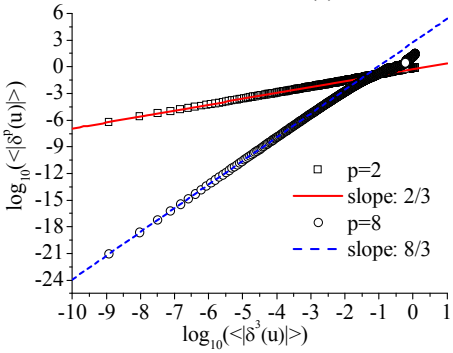

(i) Newtonian fluid case

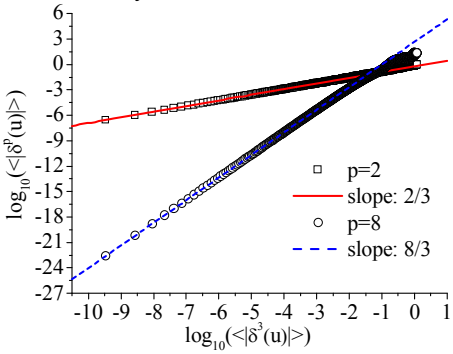

(ii) Polymer solution case

(d) Forcing homogeneous isotropic turbulence

Fig. 3 Log-log plot of $S_p(r)$ vs $S_3(r)$ showing extended self-similarity

reduced flows by viscoelastic additives is the broadening of small scale at which $\delta u(r) \propto r$, which is directly related with the smoothing effect of viscoelasticity on velocity fluctuations at scales similar to the chain length of shear induced structures formed in viscoelastic fluids. On the other hand, it is also imaginable that the broadening of small scale at which $\delta u(r) \propto r$ (Fig. 2) could be one of the reasons of the broadening of the region at which $S_p(r) \propto S_3(r)^{p/3}$ in the ESS-fashioned plots (Fig. 3). Further more, the extension of the region of $\delta u(r) \propto r$ or $S_p(r) \propto S_3(r)^{p/3}$ might provide us some clues in developing the unique numerical simulation models (such as sub-grid scale models for large eddy simulation) for drag-reducing flow by additives. All of these give us further motivations and call for further detailed studies.

CONCLUSIONS

DNS study has been carried out for drag-reduced channel flow of surfactant solution and FHIT with polymer additives. The scaling properties in such turbulent flows influenced by drag-reducing additives have been investigated. It has been obtained that the range of small scale r at which $\delta u(r) \propto r$ is enlarged in all the viscoelastic fluid cases as compared with their Newtonian fluid counterparts, which is linked with the smoothing effect of drag-reducing additives on velocity fluctuations in turbulence. In the ESS-fashioned plots of $\log_{10}(S_p(r))$ versus $\log_{10}(S_3(r))$, the region at which $S_p(r) \propto S_3(r)^{\zeta(p)}$ with $\zeta(p) = p/3$ is also broadened in viscoelastic fluids. These findings are helpful in further understanding DR mechanism and developing numerical simulation models unique for drag-reduced turbulent flow.

ACKNOWLEDGMENTS

We thank Prof. B. Yu of China University of Petroleum (Beijing) and Dr. Y. Yamamoto of Kyoto University for their discussions on DNS. This study was supported by National Natural Science Foundation of China (Grant No.10872060) and Program for New Century Excellent Talents in University of China (Grant No. NCET-07-0235). The authors are very grateful to the enthusiastic help of all members of Complex Flow and Heat Transfer Laboratory of Harbin Institute of Technology.

REFERENCES

[1] Benzi, R., Ciliberto, S., Tripiccione, R., Baudet, C., Massaioli, F. and Succi, S., 1993, "Extended self-similarity in turbulent flows", Phys. Rev. E, 48, pp. R29-R32.

[2] Benzi, R., Ciliberto, S., Baudet, C. and Chavarria, G.R., 1995, "On the scaling of three-dimensional homogeneous and isotropic turbulence", Physica D, 80, pp. 385-398.

[3] Benzi, R., Biferale, L., Ciliberto, S., Struglia, M.V. and Tripiccione, R., 1996, "Generalized scaling in fully developed turbulence", Physica D, 96, pp. 162-181.

[4] Virk, P.S., 1975, "Drag reduction fundamentals", AIChE J., 21, pp. 625-656.

[5] Sreenivasan, K.R. and White, C.M., 2000, "The onset of drag reduction by dilute polymer additives, and the maximum drag reduction asymptote", J. Fluid Mech., 409, pp. 149-164.

[6] Li, F.-C., Kawaguchi, Y., Segawa, T. and Hishida, K., 2005, "Reynolds-number dependence of turbulence structures in a drag-reducing surfactant solution channel flow investigated by particle image velocimetry", Phys. Fluids, 17, 075104.

[7] Rogallo, R.S., 1981, "Numerical experiments in homogeneous isotropic turbulence", Technical Report No.81315, NASA.

[8] Yu, B., Kawaguchi, Y., 2003, "Effect of Weissenberg number on the flow structures: DNS study of drag-reducing flow with surfactant additives", Int. J. Heat Fluid Flow, 24, pp. 491-499.

[9] Yu, B., Li, F.-C., Kawaguchi, Y., 2004, "Numerical and experimental investigation of turbulent characteristics in a drag-reducing flow with surfactant additives", Int. J. Heat Fluid Flow, 25, pp. 961-974.

[10] Yu, B., Kawaguchi, Y., 2006, "Parametric study of surfactant-induced drag-reduction by DNS", Int. J. Heat Fluid Flow, 27, pp. 887-894.

[11] Vaithianathan, T., Robert, A., Brasseur, J.G. and Collins, L.R., 2006, "An improved algorithm for simulating three-dimensional, viscoelastic turbulence", J. Non-Newtonian Fluid Mech., 140, pp. 3-22.

[12] Canuto,C., Hussaini, M.Y., Quarteroni, A. and Zang, T.A., 1988, "Spectral methods in fluid dynamics", Spring-Verlag, New York.

[13] Vaithianathan, T. and Collins, L.R., 2003 "Numerical approach to simulating turbulent flow of a viscoelastic polymer solution", *J. Compt. Phys.,* 187, pp. 1-23.

[14] Perlekar, P., Mitra, D. and Pandit, R., 2006, "Manifestations of drag reduction by polymer additives in decaying, homogenous, isotropic turbulence", *Phys. Rev. Letts.*, 97 (264501), pp. 1-4.

[15] She, Z.S., Jackson, E. and Orszag, S.A., 1991, "Statistical aspect of vortex dynamics in turbulence," in New Perspectives in Turbulence, edited by Sirovich, L., Springer-Verlag, Berlin, Chap. 12.

[16] Chen, S.Y., Doolen, G.D., Kraichnan, R.H. and She, Z.S., 1993, "On statistical correlations between velocity increments and locally averaged dissipation in homogeneous turbulence", Phys. Fluids, A 5(2), pp. 458-463.